Polymer 51 (2010) 5229–5235

Contents lists available at ScienceDirect

Polymer

journal homepage: www.elsevier.com/locate/polymer

Linear viscoelastic behavior of poly(ethylene terephtalate) above T_g amorphous viscoelastic properties Vs crystallinity: Experimental and micromechanical modeling

Fahmi Bédoui*, Michèle Guigon

Université de Technologie de Compiègne, Laboratoire Roberval UMR-CNRS 6253, Compiègne, France

ARTICLE INFO

Article history:
Received 1 June 2010
Received in revised form
25 August 2010
Accepted 30 August 2010
Available online 6 September 2010

Keywords:
Semicrystalline polymers
Amorphous confinement
Micromechanical modeling

ABSTRACT

Linear viscoelastic behavior of amorphous and semicrystalline poly(ethylene terephtalate), (PET), was experimentally investigated. PET's samples with different crystallinities (Xc) were prepared and viscoelastically characterized. Based on our experimental results (properties of the amorphous PET and semicrystalline polymers), micromechanical model was used to, first predict the viscoelastic properties of the semicrystalline polymers and second predict the changes on the viscoelastic properties of the amorphous phase when the crystallinity increases. For the micromechanical modeling of semicrystalline material's viscoelastic properties, difficulties lie on the used numerical methods (Laplace-Carson transformation) and also on the actual physical and mechanical properties of the amorphous phase. In this paper we tried to simplify the Laplace-Carson-based method by using a pseudo-elastic one that avoids the numerical difficulties encountered before. The time-dependant problem is so replaced by a frequency-dependant set of elastic equations. Good agreement with low crystallinity fraction was found however large discrepancies appear for medium and high crystallinity. The poor agreement raises the issue of which amorphous mechanical properties should be taken as input in the micromechanical model? According to the dynamic mechanical analysis (DMA) experimental data, multiple amorphous phases with different glass transition temperatures were observed for each tested semicrystalline sample. For each sample, new glass transition temperature related to an equivalent amorphous phase was determined. DMA tests done at 1 Hz help estimating the mechanical properties of the new amorphous phase based on its new glass transition temperature. Using the new micromechanical approach developed in this paper, the changes occurring on the viscoelastic behavior of the amorphous phase upon crystallization were estimated. Good agreement was found after comparing the micromechanically estimated amorphous behavior with the experimentally estimated one leading to believe that the physical and mechanical properties of the amorphous phase change upon crystallization and taking on account this phenomenon is a key to a good prediction of the semicrystalline behavior using micromechanical models.

1. Introduction

Polymer materials are increasingly used in industrial parts. It is true for both, semicrystalline and amorphous polymers which are widely used as structural materials in critical functions. These new applications make, technologically and academically, mandatory to understand their behavior under complex conditions (chemical environment, stress field… etc.). Monitoring the behavior of these materials *in-situ* and *ex-situ*, to investigate the different mechanisms at different length scales should help building robust behavior laws that could be used in dimensioning new structures using polymer materials. A multiscale description of the structure, i.e., a representation of the structure and morphology at several length scales (from micro-scale down to nano-scale), is the currently favored approach. However, valid prediction of the materials properties by any of the current models requires precise description of the relevant structural parameters. Focus should be beyond standard microstructural characterization in term of phase fraction, mechanical measurements and computational modeling. More interest should be attached on the interconnection of the constituent phases and how that could affect their respective physical and/or mechanical properties.

Micromechanical models were thoroughly used to predict mechanical properties of semicrystalline polymers (plastic behavior) [1–9]. Recently the prediction of the elastic behavior was subject to

* Corresponding author. Tel.: +33 3 44 23 45 28; fax: +33 3 44 23 49 84.
E-mail address: fahmi.bedoui@utc.fr (F. Bédoui).

0032-3861/$ – see front matter © 2010 Elsevier Ltd. All rights reserved.
doi:10.1016/j.polymer.2010.08.058

an intense interest either to estimate macroscopic properties [9–14] or try to shed some light on some paradoxes behavior in polyolefin polymers (polyethylene and polypropylene) [15]. However difficulties on applying micromechanics to predict viscoelastic behavior of semicrystalline polymer still not overcome. In previous work both amorphous and semicrystalline PET were characterized [12,16]. X-ray data allowed the determination of the shape ratio of crystalline phase. Different micromechanical models were used to estimate the viscoelastic behavior of the semicrystalline polymer [16]. For low crystallinity, good agreement was found however large discrepancy was found for higher crystalline fraction. The discrepancy modeling/experiment was attributed to the possible effect of confinement of the amorphous phase due to the presence of the crystalline phase. In a recent paper dealing with elastic behavior of PET, an inter-phase with different mechanical properties was introduced to help predict the macroscopic mechanical properties of the semicrystalline polymers. This new inter-phase was justified based on previous work [17] assuming a possible change that could affect the mechanical properties of the PET's amorphous phase upon crystallization. However no experimental techniques had mechanically quantified that effect.

In this paper combining viscoelastic DMA characterization and simplified viscoelastic micromechanical modeling, we tried to shed light on the effect of crystallization on the mechanical properties of the amorphous phase.

Unlike elasticity, viscoelastic behavior assumes an evolution of the mechanical properties (Young's modulus e.g.) Vs. time. This dependence could not be taken on account using standard micromechanical models. Numerical techniques were introduced to help solving this issue. For composite materials Schapery [18] proposed to use the collocation method coupled with Laplace-Carson transformation and inversion tool. In a recent study Rekik and Brenner [19] introduces a constraints collocation method to predict composite materials behavior. The same concept, based on constraints coupled with the collocation method were used for semicrystalline polymer, shows the limit of the micromechanics model to fit the viscoelastic behavior of semicrystalline polymers [16]. The numerical difficulties due to the Laplace-Carson inversion and numerical inversion coupled with suspicion of the changes that occurs on the mechanical properties of the amorphous phase makes difficult the interpretation of the results.

In this paper we, *first* focus on simplifying the numerical method by replacing the Laplace-Carson transformed problem by a frequency-dependant one based on the use of the complex modulus instead of the storage and loss ones. In other word the time-dependant problem will be replaced by a frequency one leading to easier problem where any elastic micromechanical model could be used. According to previous results [12] the differential scheme is well suited to predict the macroscopic properties of such materials. More details about the micromechanical model could be found in previous work [12,15]

Second, based on the DMA results, the changes, in term of mechanical behavior, occurring in the both amorphous and semicrystalline polymers behavior will be correlated to the prediction given by the micromechanical model. It appears that the glass transition of the amorphous phase changes upon the increase of the crystallization leading to a shift in the actual behavior of the amorphous phase (T_g and Tan(δ)). The increase of the T_g could be explained as the signature of the confinement effect. That effect was not taken on account in mechanical properties of the amorphous phase and lead to the discrepancies model-experiment in previous work [16].

2. Experiment and results

2 mm thick PET Extruded plate from ISO-SUD was used in this study. Samples were cut as rectangular stripes (easy to be used for DMA experiments) and annealed at T = 110 °C for different period of time. Three crystallinities were prepared (17, 24 and 35%). DSC run were carried out to determine the crystallinity of each sample. From the total area of the exothermic and the endothermic peaks crystallization and fusion enthalpy were determined. For crystallinity calculation purposes melting enthalpy of fully crystalline PET is $\Delta H^*_{mc} = 117.6\ J/g$ [20] along with densities of pure amorphous and crystals ($\rho_c = 1.445\ g\,cm^{-3}, \rho_c = 1.335\ g\,cm^{-3}$) [21] were used. DMA tests using a METRAVIB DMA 150 machine were conducted over four decades (0.01–100 Hz) at 90 °C to ensure being above the glass transition temperature of the amorphous phase of PET (replacing semicrystalline polymer) ($T_g \approx 80$ °C). Fig. 1 presents the DMA results for the four samples (amorphous and crystalline). Amorphous and low crystallinity sample (17%) polymers undergo a parabolic dependence of the complex modulus vs. the frequency. However for frequencies between 0.1 Hz and 10 Hz, the medium and high crystallinity samples (24 and 35%) show steep modulus shape.

To investigate this effect, temperature sweep at 1 Hz dynamic excitation experiments were conducted on the four different samples. The tan(δ) Vs. temperature presented in Fig. 2 confirms a different viscoelastic behavior between in one hand amorphous and low crystallinity (Xc = 17%) samples and on the other the hand medium and high crystallinity ones (24 and 35%).

For amorphous as for the 17% crystallinity a major peak appear around 84 °C that could be considered as the T_g temperature and a minor peak at higher temperature. For Xc = 24% and Xc = 35% the tan(δ) graph shows clearly two different peaks. Origin software [22] was used to deconvolute the peaks. Peaks are considered Gaussian. In order to perform the deconvolution operation we are supposed to introduce the baseline parameters. In our case, for all the samples, a fourth order polynomial function was used as baseline (see Fig. 3).

It appears for amorphous and low crystallinity the major peak is around 84 °C (T_g of the pure amorphous polymer) and a minor peak at 92 °C. For Xc = 24% the two peaks, almost with equal weight, are at 84 °C and 96.6 °C respectively. For the highest crystallinity, (35%) the first peak, the minor one in this case, is around 86 °C and the second one appears around 99.5 °C.

The presence of two peaks in the Tan(δ) Vs. temperature graphs could be explained as a coexistence of two amorphous phases with different glass transition temperatures [23]. In semicrystalline polymer speculation about two different amorphous phases (free and constrained) were discussed in previous papers [14,17,24]. Upon annealing above T_g, crystalline lamellae

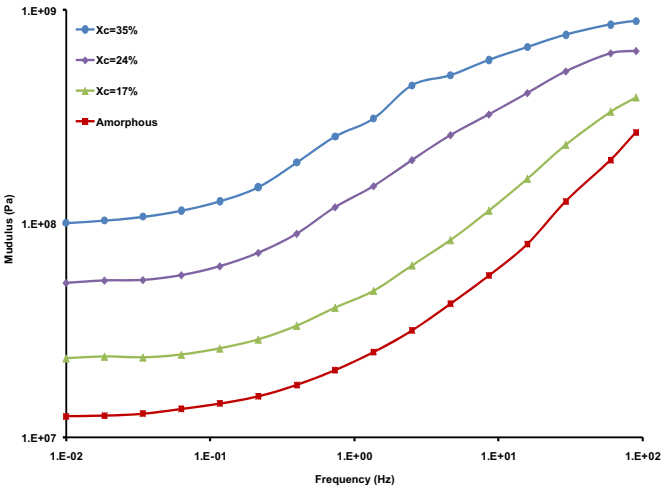

Fig. 1. DMA data for amorphous and semicrystalline polymers.

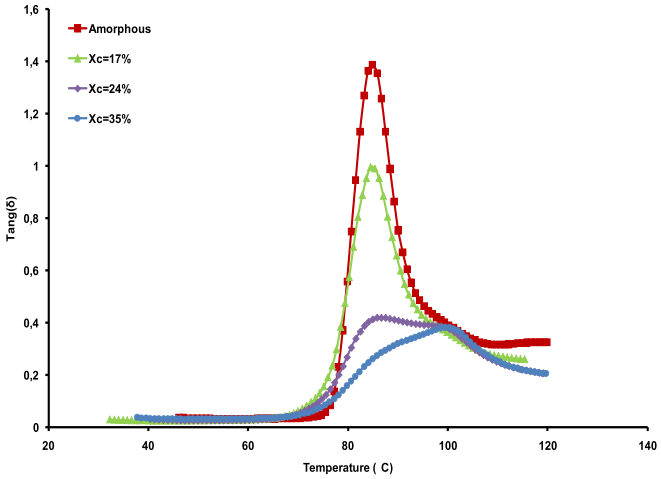

Fig. 2. Effect of crystallinity on the viscoelastic behavior of amorphous and semicrystalline polymers (tests done at 90 °C).

start growing in the pure amorphous matrix. The presence of the crystalline phase contributes to the restriction of the mobility of the amorphous regions [25]. This restriction appears as an increase in the relaxation time of the segmented molecular chains [17,26] and a decrease in the interchain distance due to change in the short-range ordering of the amorphous chain segments [27]. Fig. 4 presents schematically, the author's view of the layout of the two phases. For low crystallinity, the crystalline lamellae start nucleating, and so the effect of confinement is negligible to affect the mobility of the chain and consequently its viscoelastic behavior. For medium crystallinity (Xc = 24%), secondary crystallization leads to more organized spherulitic structure. At an intraspherulitic structure, the confinement effect increases and contribute to a drastic mobility restriction. The T_g-shift, as seen in the second peak of Tan(δ) graph, is suspected to be the signature of this effect. For higher crystallinity, increase in crystallinity combined with the perfection of the secondary crystallization phenomena lead to mobility restriction at both intra and interspherulitic scale. Both amorphous phases lying in and between spherulites will be subject to the confinement effect leading to a shift of the two peaks (Figs. 2 and 3) as it appears for the 35% crystallinity sample.

Based on the deconvolution results, the area of each peak was determined and using the Fox Law [28] an equivalent glass transition temperature was determined, the results are summarized in the Table 1.

3. Discussion

Semicrystalline polymer is considered as heterogeneous material at nano-length-scale. In fact for PET, nanometeric length crystalline lamella starts growing when annealing amorphous samples above T_g. At low crystallinity rate the crystals are embedded in a pure-like amorphous matrix. For medium and higher crystallinity, spherulites, (more organized structure) start taking place. To predict the mechanical behavior (elastic, plastic and viscoelastic) of semicrystalline polymer, the isotropic spherulitic structure complexity is difficult to be taken on account. The spherulitic microstructure will be idealized as anisotropic crystalline phase embedded in an isotropic amorphous phase. Previous work [12,15] proved that among the available micromechanical models, the differential scheme is well adapted for such materials. In this case the crystal lamellae are dispersed randomly in an amorphous matrix, the crystalline phase, considered here as reinforcing inclusion, will be introduced with small increments assuming that

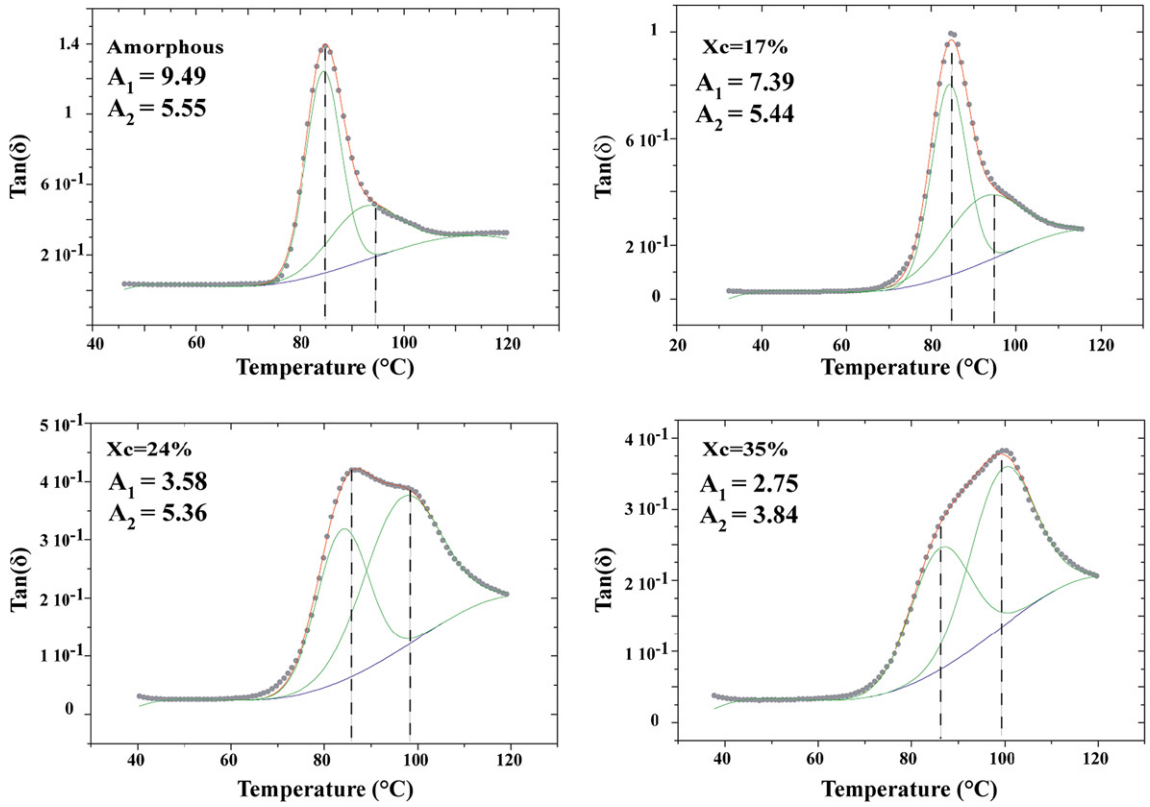

Fig. 3. Deconvolution of Tan(δ) peaks for amorphous and semicrystalline polymers.

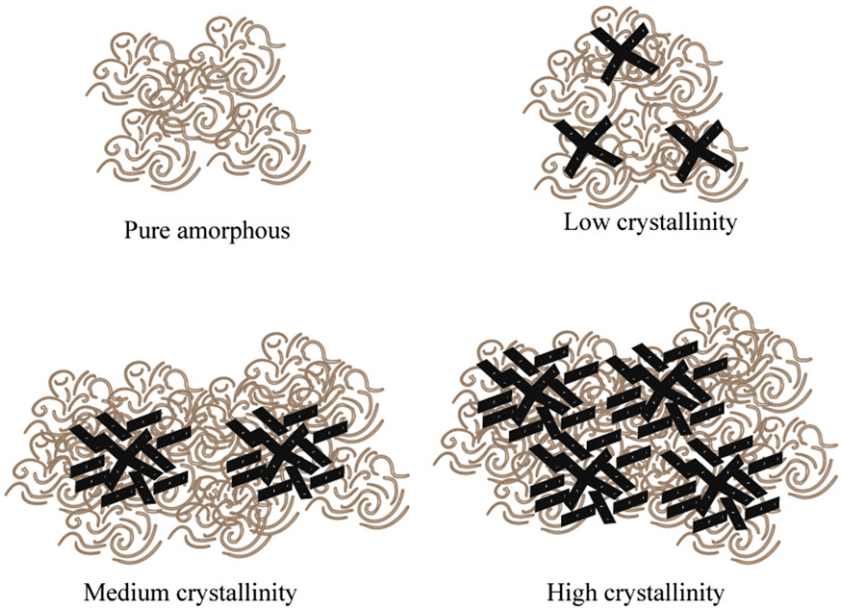

Fig. 4. Schematic representation of the layout of the crystalline and the amorphous phase for amorphous and semicrystalline polymers.

the dilute-distribution assumption is valid at each step [29]. At the first increment the matrix surrounding the inclusions is the amorphous phase, at the following increments, the matrix surrounding the inclusions is characterized by a uniform behavior (elastic, thermoelastic or viscoelastic), which has been calculated at the previous increment (Fig. 5).

For semicrystalline polymers, such model shows a good agreement with experimental results in the case of elasticity [12,15]. For viscoelasticity poor agreement model-experiments was found. The used numerical method (Laplace-Carson inversion) and the mechanical properties of the amorphous phase (used as input in the model) were suspected to be the origin of the discrepancies [16]. Indeed to predict the viscoelastic behavior using differential scheme we had to, at each step, transform the time-dependant problem in the Laplace-Carson space. The time-dependant problem will be, so replaced by an equivalent elastic one, easy to be solved by any micromechanical model. A numerical inversion tool will be needed to get back to the time space. Different numerical methodologies could be used like collocation method [18], direct method [30] or multi-data method [16]. The numerical difficulties related to the cited methods prevent any critical material-related questioning of the predicted results. This is more critical in the case of poor agreement experiments-modeling. So, decoupling the effect of the numerical incertitude due to the inversion method from the incoherence of the initial amorphous input data become difficult to be judged.

Table 1
Materials and Tg-shift based on the deconvolution's results.

Polymers	Amorphous		Xc = 17%		Xc = 24%		Xc = 35%	
	1st	2nd	1st	2nd	1st	2nd	1st	2nd
Tg at each peak (°C)	84	92	84	92	84	96.6	86	99.5
Area of peaks (AU[a])	9.49	5.55	7.39	5.45	3.58	5.36	2.75	3.84
$T_{g\text{-shift}}$ (°C)	86.9		87.4		91.15		93.15	

[a] Arbitrary unit.

To overcome this issue, we propose to simplify the prediction method as the following. Based on the DMA results instead of representing the viscoelastic behavior in term of Elastic (E') and loss modulus (E") we will consider the complex modulus E*. E* is related to E' and E" using the following equations:

$$E^* = E' + iE''$$

$$\|E^*\| = \sqrt[2]{E'^2 + iE''^2}$$

where i stands for the complex argument.

According to the previous equation, instead of having a time-dependant modulus, we will have frequency-dependant ones. At each frequency an elastic problem should be solved using the differential scheme.

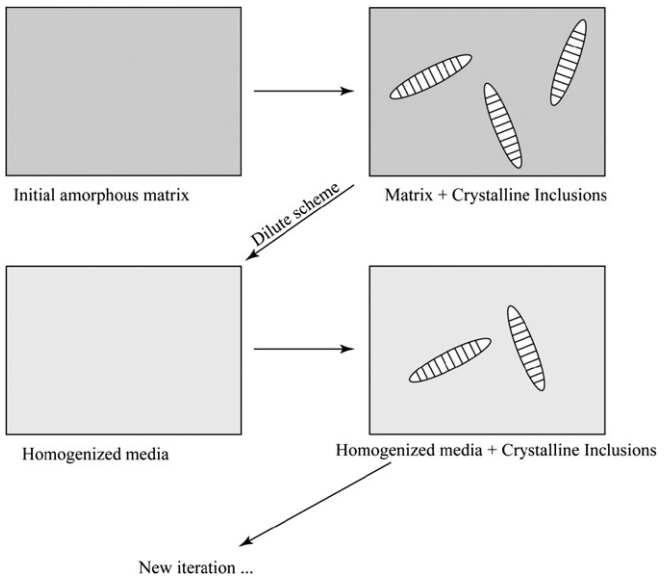

Fig. 5. Schematic representation of the used micromechanical model (differential scheme).

$$C_n^h(\Omega) = C_{n-1}^h(\Omega) + \delta x\left(C^c - C_{n-1}^h(\Omega)\right) : A^n$$

$$A^n(\Omega) = I + S_{n-1}^{esh} C_{n-1}^{-1}(\Omega)\left(C^c - C_{n-1}^h(\Omega)\right)$$

where C^c is the crystalline rigidity tensor, S^{esh} is the Eshelby tensor, I is the fourth order identity tensor, $C_n^h(\Omega)$ is the equivalent homogeneous field rigidity tensor at the nth step for the defined frequency Ω ($\Omega = 2\pi f$, f is the frequency). For the first step $C_{n-1}^h(\Omega)$ will be the amorphous rigidity tensor. Amorphous phase will be considered isotropic. At each frequency the amorphous rigidity tensor will be built based on the complex modulus and Poisson's coefficient ν. The Poisson coefficient was determined after calculating the bulk modulus from the PVT data ($K = -1/\nu(\mathrm{d}\nu/\mathrm{d}p)$). At 90 °C the bulk modulus is 2845 MPa. The bulk modulus will be considered frequency independent. The crystalline inclusion, considered as reinforcement phase, has approximately a cubic-like shape. Shape ratios were determined in previous work [12]. In this paper a shape ratio of 2:2:1 will be used. Mechanically, the crystalline phase is anisotropic [31–33]. The rigidity tensor is as follow:

$$C^{\mathrm{PET}} = \begin{pmatrix} 7.7 & 5.46 & 5.07 & 0 & 0 & 0 \\ 5.46 & 7.7 & 5.07 & 0 & 0 & 0 \\ 5.07 & 5.07 & 118 & 0 & 0 & 0 \\ 0 & 0 & 0 & 1.62 & 0 & 0 \\ 0 & 0 & 0 & 0 & 1.62 & 0 \\ 0 & 0 & 0 & 0 & 0 & 1.12 \end{pmatrix} \mathrm{GPa}$$

The differential scheme was used to estimate the macroscopic behavior of the low crystallinity sample. Unsurprisingly, a good agreement between modeling and experiment was found as presented in Fig. 6. Indeed, as for previous work, micromechanical modeling was able to catch the viscoelastic behavior of low crystallinity polymers.

However for medium and higher crystallinity the estimation is far from the experimental results (Figs. 7 and 8). According to DMA results, the discrepancies could be attributed to the change in the amorphous phase properties after crystallization took place. In a recent paper Diani et al. raises this issue based on DMA experiments performed slightly under T_g (70 °C) for PET material. The same issue was encountered at a higher length-scale (PET amorphous matrix filled with spherical glass beads), Cruz et al. [34] when trying to model the viscoelastic properties of the composite materials. For the cited references [16,34], as input for the modeling, each phase was identified (elastic for crystalline phase or glass beads and viscoelastic for amorphous PET phase). For both nano and micro length-scale, authors [16,34] barge into difficulties fitting experimental data with micromechanical models for both low (below T_g) and high temperature (above T_g). The differences between experimental data and theoretical estimation were attributed to a possible "confinement" effect of the amorphous phase. These results (actual work and literature results) strengthen the author's believe that the identified amorphous properties stand only for pure or low crystallinity samples. For medium and high crystallinity the identified amorphous properties is no longer valid to be used as an input data for micromechanical modeling.

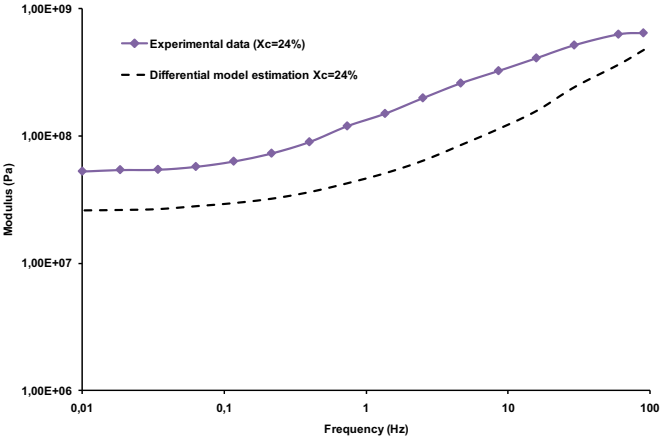

Fig. 7. Estimation of the complex modulus for Xc = 17%.

To quantify the effect of the presence of the crystalline phase on the amorphous mechanical properties, a reverse calculation was conducted. Using the differential micromechanical scheme, for each frequency knowing the macroscopic modulus and the crystalline rigidity, the amorphous phase modulus was determined by minimizing the following equation:

$$\underset{\Omega}{\mathrm{Min}}\left[\tilde{C}^n\left(\tilde{C}_{am}, \Omega\right) - C^n(C_{am}, \Omega)\right]$$

Where C_{am} is the initial amorphous rigidity, C^n is the equivalent homogeneous field rigidity tensor at the nth step, $\tilde{C}_{am}$ is the actual amorphous rigidity $\tilde{C}^n$ is the equivalent homogeneous field rigidity based on the $\tilde{C}_{am}$.

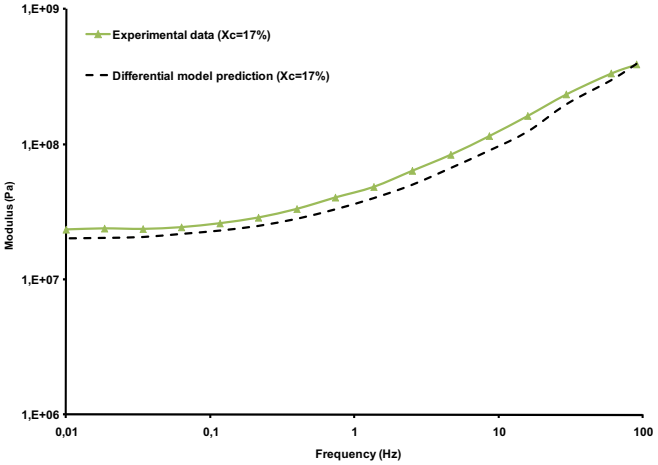

Fig. 6. Estimation of the viscoelastic modulus for the low crystalline fraction sample (Xc = 17%).

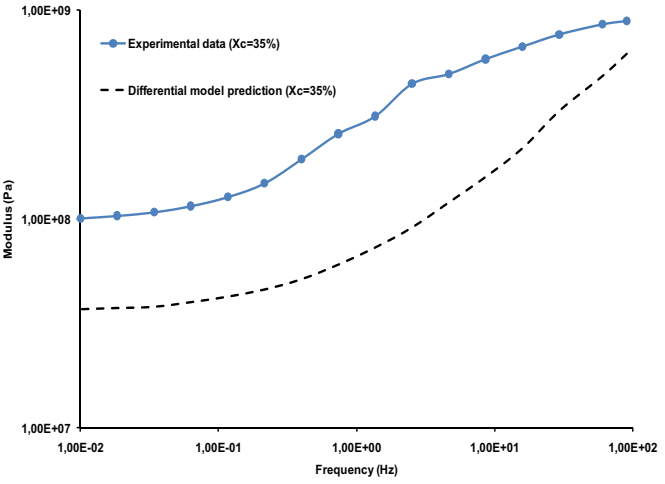

Fig. 8. Estimation of the complex modulus for Xc = 35%.

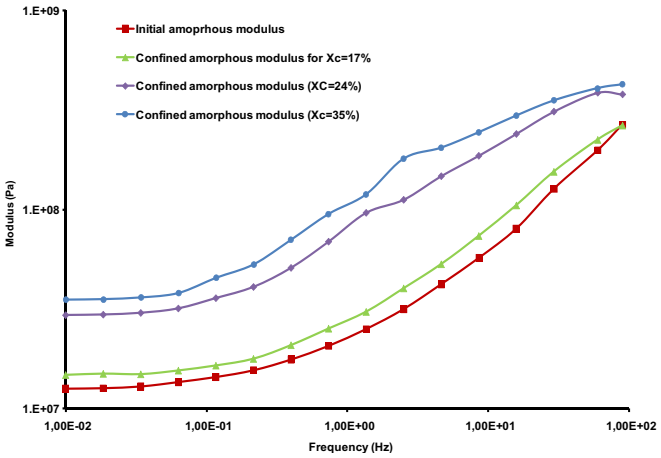

Fig. 9. confinement effect on the amorphous phase properties.

Based on the explained methodology, the effect of the confinement was determined. For each sample, the equivalent amorphous modulus was determined for the considered frequencies. For low crystalline polymer, unsurprisingly, the effect of the confinement was negligible. However a drastic increase was found for the other sample Xc = 24 and 35% (Fig. 9).

The difficulty lies on the validity of the found modulus. No direct experimental techniques could allow the measurement of the actual mechanical properties of the amorphous phase after the samples are crystallized. Nevertheless based on the results presented on the Table 1, the T_g-shift given by the deconvolution of the tan(δ) graphs could be used to validate the micromechanical result. In fact at 90 °C, if we consider the T_g of the pure amorphous polymer as the reference glass transition temperature (T_g = 86.9 °C, see table one) for the crystalline polymer, the amorphous phase lying between crystals and spherulites would have an equivalent T_g-shifted by:

- 0.43 °C for Xc = 17%,
- 4.2 °C for Xc = 24%,
- 6.5 °C for Xc = 35%.

So the amorphous phase lying between crystalline lamellae should have a modulus of an equivalent pure amorphous phase (for which the T_g is equal to 84 °C) at a temperature equal to $T_g - T_g$-shift. At 90 °C the amorphous phase of the semicrystalline samples, will behave as an equivalent pure amorphous PET at 83.6 °C for Xc = 17%, and 80.8 °C for Xc = 24%, and 77.5 for Xc = 35%. According to temperature sweep experiments done at 1 Hz, the mechanical properties of the amorphous PET at the specified temperature were compared to the predicted confined amorphous modulus at 1 Hz solicitation (Fig. 10).

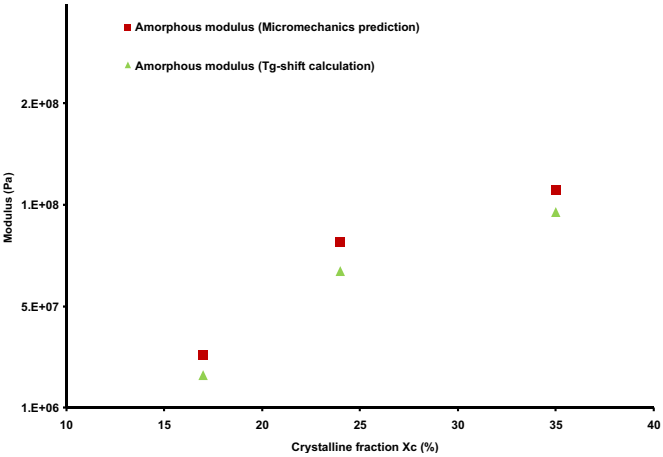

Fig. 10. Micromechanical modeling Vs. Tg-shift based modulus for semicrystalline polymers.

An acceptable agreement was found between the micromechanical modeling and the T_g-shift based amorphous modulus. This result could be considered a mixture of modeling experimental method to confirm the effect of the confinement on the amorphous viscoelastic properties.

4. Conclusion

Viscoelastic behavior of amorphous and semicrystalline polymers was characterized using DMA techniques. The effect of crystallization on the amorphous properties was investigated. A new simplified methodology in dealing with viscoelastic micromechanical modeling was presented. Based on micromechanical models correlation between crystallinity and changes on the T_g of the amorphous properties were discussed. This work helps shedding some light on both physical and numerical difficulties encountered in prediction mechanical properties of semicrystalline polymers. Indeed the use of the micromechanical model predicting viscoelastic properties of materials was simplified by replacing the time-dependant problem by an elastic simplified one. Using this methodology, physical aspects suspected but ignored in previous work was investigated and more understood. In future work the thermoelastic properties of semicrystalline and amorphous phase will be investigated.

Acknowledgment

The authors acknowledge the financial support of the Mechanical Engineering Department of the Université de Technologie de Compiègne for this study, under the contract No M117L.

References

[1] Dahoun A, Aboulfaraj M, G'Sell C, Molinari A, Canova GR. Polymer Engineering & Science 1995;35(4):317–30.
[2] G'Sell C, Dahoun A. Materials Science and Engineering: A 1994;175 (1–2):183–99.
[3] Lee BJ, Argon AS, Parks DM, Ahzi S, Bartczak Z. Polymer 1993;34(17):3555–75.
[4] Lee BJ, Parks DM, Ahzi S. Journal of the Mechanics and Physics of Solids 1993;41(10):1651–87.
[5] Nikolov S, Doghri I, Pierard O, Zealouk L, Goldberg A. Journal of the Mechanics and Physics of Solids 2002;50(11):2275–302.
[6] van Dommelen JAW, Parks DM, Boyce MC, Brekelmans WAM, Baaijens FPT. Journal of the Mechanics and Physics of Solids 2003;51(3):519–41.
[7] van Dommelen JAW, Parks DM, Boyce MC, Brekelmans WAM, Baaijens FPT. Polymer 2003;44(19):6089–101.
[8] Makradi A, Ahzi S, Gregory RV, Edie DD. International Journal of Plasticity 2005;21(4):741–58.
[9] Spieckermann F, Wilhelm H, Schafler E, Ahzi S, Zehetbauer MJ. Materials Science and Engineering: A 14th International Conference on the Strength of Materials 2008;483–484:76–8.
[10] Ahzi S, Bahlouli N, Makradi A, Belouettar S. Journal of Mechanics of Materials and Structures 2007;2(1):1–21.
[11] Ahzi S, Parks DM, Argon AS. American Society of Mechanical Engineers, Applied Mechanics Division, AMD 1995;203:31–40.
[12] Bédoui F, Diani J, Régnier G, Seiler W. Acta Materialia 2006;54(6):1513–23.
[13] Guan X, Pitchumani R. Polymer Engineering and Science 2004;44(3):433–51.
[14] Gueguen O, Ahzi S, Makradi A, Belouettar S. Mechanics of Materials 2010;42 (1):1–10.
[15] Bédoui F, Diani J, Régnier G. Polymer 2004;45(7):2433–42.
[16] Diani J, Bédoui F, Régnier G. Materials Science and Engineering: A 2008;475 (1–2):229–34.
[17] Arnoult M, Dargent E, Mano JF. Polymer 2007;48(4):1012–9.
[18] Schapery RA. On the characterization of nonlinear viscoelastic materials. 9; 1967. pp. 295–310.
[19] Rekik A and Brenner R. AFM, Maison de la Mécanique, 39/41 rue Louis Blanc – 92400 Courbevoie; 2007.
[20] Göschel U. Polymer 1996;37(18):4049–59.

[21] Xu T, Bin Y, Nakagaki Y, Matsuo M. Macromolecules 2004;37(18):6985–93.
[22] OriginPro. Origin 7.0. In: SR0 OLC, editor. Northampton, MA: Origin-Lab-Corporation, 1991–2002.
[23] Shieh YT, Lin YS. Journal of Applied Polymer Science 2009;113(5):3345–53.
[24] Righetti MC, Tombari E, Angiuli M, Lorenzo MLD. Thermochimica Acta 2007;462(1–2):15–24.
[25] Illers KH, Breuer H. Journal of Colloid Science 1963;18(1):1–31.
[26] Sefcik MD, Schaefer J, Stejskal EO, McKay RA. Macromolecules 1980;13(5):1132–7.
[27] Murthy NS, Correale ST, Minor H. Macromolecules 1991;24(5):1185–9.
[28] Fox TG. Bulletin of the American Physical Society 1956;1:123.
[29] McLaughlin R. International Journal of Engineering Science 1977;15(4):237–44.
[30] Brenner R, Masson R, Castelnau O, and Zaoui A. European Journal of Mechanics – A/Solids;21(6):943–960.
[31] Hine PJ, Ward IM. Journal of Materials Science 1996;31(2):371–9.
[32] Rutledge GC. Macromolecules 1997;30(9):2785–91.
[33] Matsuo M, Sawatari C. Polymer Journal 1990;22(6):518–38.
[34] Cruz C, Diani J, Régnier G. Composites Part A: Applied Science and Manufacturing 2009;40(6–7):695–701.